2015 European Control Conference (ECC)
July 15-17, 2015. Linz, Austria

Control of a Biomass-Furnace Based on Input-Output-Linearization

Christoph Schörghuber[1], Markus Reichhartinger[1], Martin Horn[1], Markus Gölles[2] and Richard Seeber[1]

***Abstract*— The operation of modern biomass combustion plants with high efficiencies and low emissions requires advanced control strategies. In this paper the controller design for a medium-scale biomass furnace based on input-output-linearization is presented. A fourth order nonlinear model with four inputs and four outputs forms the basis for controller design. Due to a time-delayed input the stabilization of the internal dynamics is challenging. Two stabilization methods are suggested and a stability analysis is given. Finally, experimental results are presented and discussed.**

I. INTRODUCTION

Due to increasing efforts to reduce CO_2-emissions biomass combustion has gained in importance over the last decades. Grate combustion is a common and well developed technology for burning solid biomass fuels. Modern grate combustion plants are optimized in geometry and consist of air staging strategies enabling low emission operation. In order to achieve low emissions at high efficiencies advanced control techniques play a decisive role.

From a system theoretic point of view a biomass boiler is a nonlinear multivariable system. In industrial state-of-the-art controllers nonlinearities and crosscouplings usually are neglected. Typically PID-controllers are designed on basis of linear, mutually decoupled SISO-systems, e.g. [1]–[3]. Due to these simplifications the full potential of the plant in terms of low emissions and high efficiencies cannot be exploited at all. Up to now just a few groups worked on the development of modern model based control strategies for biomass furnaces, e.g. [4]–[7]. Several approaches deal with model predictive control of medium- and large-scale biomass furnaces, e.g. [5]–[7].

The approach outlined in this paper is based on the well known input-output-linearization technique, e.g. [8]–[10]. To design the controller special attention has to be paid to the internal dynamics of the linearized and decoupled plant. Due to time-delay in the system the stabilization of the internal dynamics is challenging. In [11], [12] this stabilization is achieved by means of a proportional controller without a rigorous proof of stability. In this paper a stability analysis is outlined for two different stabilization methods on basis of a medium-scale biomass furnace with a horizontally moving grate and a hot water boiler (nominal capacity: 180kW).

The paper is organized as follows: In section II a description of the plant is given and in section III a mathematical model is presented. Section IV outlines the controller design and discusses the stabilization of the internal dynamics. In section V simulation and experimental results are presented and finally in section VI a conclusion is given.

[1]Christoph Schörghuber, Markus Reichhartinger, Martin Horn and Richard Seeber are with the Institute of Automation and Control, Graz University of Technology, Graz, Austria christoph.schoerghuber@tugraz.at

[2]Markus Gölles is with the competence centre BIOENERGY 2020+ GmbH, Graz, Austria markus.goelles@bioenergy2020.eu

II. PLANT DESCRIPTION

A schematic overview of a medium-scale biomass furnace with a horizontally moving grate and a fire tube hot water boiler (nominal capacity: 180kW) is shown in Fig. 1. The combustion process is sub-divided into two zones, the primary and the secondary combustion zone, each with separate air supply. Via the fuel screw conveyor biomass (typically wood chips) enters the primary combustion zone, where the combustion is provided with primary air flowing from below the grate. Due to air staging strategies only a certain part of the air massflow required for complete combustion is supplied via the primary air. At the beginning of the secondary combustion zone secondary air is injected with high velocities to get a homogeneous mixture of the still combustible flue gas and oxygen leading to a complete combustion with low emissions. The hot flue gas then enters the heat exchanger (hot water boiler) where most of the thermal energy is transferred to water. Finally, the cooled flue gas is routed to the chimney from where a certain part is recirculated into the primary combustion zone in order to reduce the combustion temperature, see Fig. 1.

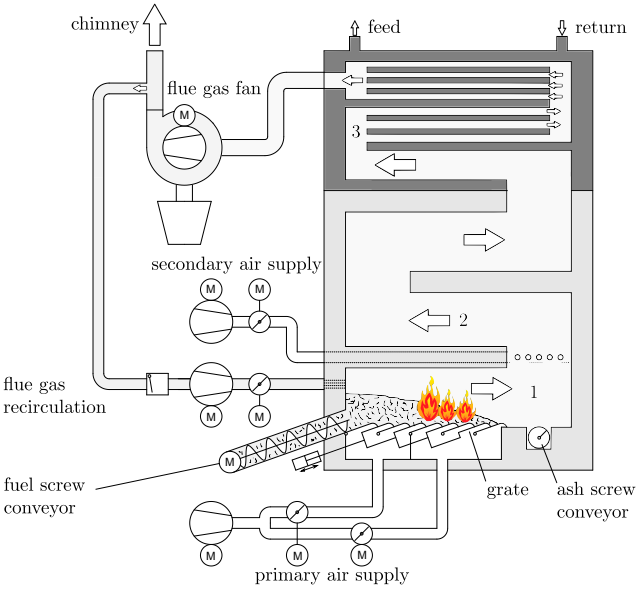

Fig. 1. Schematic overview of a medium scale biomass furnace (1 primary combustion zone, 2 secondary combustion zone, 3 hot water boiler)

The combustion process can be influenced by the fed fuel- $\dot{m}_{\mathrm{ff}}$, the primary air- $\dot{m}_{\mathrm{pa}}$, the secondary air- $\dot{m}_{\mathrm{sa}}$ and the recirculated flue gas-massflow $\dot{m}_{\mathrm{rf}}$. These massflows represent the four actuating signals. In [13] a method to control the air and flue gas massflows via fans and flaps is presented. Variables to be controlled are the oxygen content of the flue gas $x_{\mathrm{O_2fg}}$, the combustion temperature in the secondary combustion zone T_{sz}, the feed temperature of the heated water T_{f} and the (non-measurable) air-ratio in the fuel bed λ_{fb} describing the ratio between supplied primary air and minimal necessary air for complete combustion. The biomass furnace therefore is a multivariable system with four inputs and four outputs.

III. MODELLING

The model used for controller design can be divided into three parts. The first part, the so called fuel bed, describes the decomposition process of biomass on the grate. Because of the high moisture content the behavior of dry fuel and water is modeled separately. The evaporation of water and the decomposition of the dry fuel is described by mass balances

$$\frac{dm_{\mathrm{w}}}{dt} = \frac{-c_{\mathrm{e}}}{1+c_{\mathrm{t}}d_1} m_{\mathrm{w}} + \frac{d_1}{1+c_{\mathrm{t}}d_1}\dot{m}_{\mathrm{ff}}(t-\tau), \tag{1a}$$

$$\frac{dm_{\mathrm{f}}}{dt} = \frac{c_{\mathrm{e}}c_{\mathrm{t}}}{1+c_{\mathrm{t}}d_1} m_{\mathrm{w}} + \frac{1}{1+c_{\mathrm{t}}d_1}\dot{m}_{\mathrm{ff}}(t-\tau) - c_{\mathrm{d}}d_2(\dot{m}_{\mathrm{pa}}+\dot{m}_{\mathrm{pa0}})m_{\mathrm{f}}, \tag{1b}$$

where m_{f} and m_{w} denote the masses of dry fuel and water respectively. Here $d_1 = \frac{w_{\mathrm{bm}}}{1-w_{\mathrm{bm}}}$ is a disturbance determined by the time-varying moisture content w_{bm} and d_2 is a disturbance describing a variable decomposition factor which averages 1. Usually these disturbances are not measurable. Note that the fuel-feed $\dot{m}_{\mathrm{ff}}$ is delayed by a variable time-delay τ. For steady-state, a simple approximation for this time-delay is given by $\tau \approx c_\tau d_1$. The positive constant parameters c_{e}, c_{t}, c_{d}, $\dot{m}_{\mathrm{pa0}}$ and c_τ can be obtained by experiments. More details on the model and the parameter estimation is given in [14]. The resulting flue gas massflow $\dot{m}_{\mathrm{fg}}$ and the flue gas temperature T_{fg} are obtained via energy and material balances and depend on the variables m_{w} and m_{f}. Additionally the oxygen content $x_{\mathrm{O_2fg}}$ of the flue gas and the air-ratio λ_{fb} in the fuel bed are calculated via material balances.

The second part of the model describes the heat exchanger. The heat exchanger is connected to a water circuit with a feed (temperature T_{f}) and a return (temperature T_{r}). The dynamics of the feed temperature can be modeled by

$$\frac{dT_{\mathrm{f}}}{dt} = \frac{d_3}{c_{\mathrm{f}}}(d_4 - T_{\mathrm{f}}) + \frac{c_{\mathrm{q}}}{c_{\mathrm{f}}c_{\mathrm{w}}}\dot{m}_{\mathrm{fg}}(T_{\mathrm{fg}} - T_{\mathrm{w}}), \tag{2}$$

with the measurable disturbance $d_3 = \dot{m}_{\mathrm{w}}$ describing the water massflow of feed and return, the measurable disturbance $d_4 = T_{\mathrm{r}}(t-\tau_{\mathrm{r}})$ describing the return temperature delayed by a variable time-delay τ_{r}, the specific heat capacity of water c_{w} and a constant average water temperature T_{w}. The time-delay τ_{r} is dependent on the water massflow $\dot{m}_{\mathrm{w}}$. The positive constants c_{f} and c_{q} are found by experiments. The flue gas massflow $\dot{m}_{\mathrm{fg}}$ and the flue gas temperature T_{fg} are the inputs of the model as it is outlined in detail in [15].

The last part of the model describes the temporal behavior of the sensor measuring the flue gas temperature T_{fg} in the secondary combustion zone. The dynamics of the sensor temperature T_{sz} is modeled via

$$\frac{dT_{\mathrm{sz}}}{dt} = \frac{1}{\tau_{\mathrm{s}}}(T_{\mathrm{fg}} - T_{\mathrm{sz}}), \tag{3}$$

where τ_{s} is the time constant of the sensor.

The overall model with the states $x_1 = T_{\mathrm{f}}$, $x_2 = T_{\mathrm{sz}}$, $x_3 = m_{\mathrm{w}}$ and $x_4 = m_{\mathrm{f}}$ and the inputs $u_1 = \dot{m}_{\mathrm{pa}} + \dot{m}_{\mathrm{pa0}}$, $u_2 = \dot{m}_{\mathrm{rf}}$, $u_3 = \dot{m}_{\mathrm{pa}} + \dot{m}_{\mathrm{sa}}$ and $u_4 = \dot{m}_{\mathrm{ff}}$ can be summarized as follows:

$$\frac{dx_1}{dt} = c_1 d_3(d_4 - x_1) + \tilde{c}_2 x_3 + \tilde{c}_3 d_2 u_1 x_4 + \tilde{c}_4 u_2 + \tilde{c}_5 u_3, \tag{4a}$$

$$\frac{dx_2}{dt} = -c_6 x_2 - \frac{c_7 x_3 - c_8 d_2 u_1 x_4 - \tilde{c}_9 u_2 - \tilde{c}_{10} u_3}{c_{11} x_3 + c_{12} d_2 u_1 x_4 + u_2 + u_3} + \tilde{c}_{13}, \tag{4b}$$

$$\frac{dx_3}{dt} = \frac{-c_{11}}{1+c_{14}d_1} x_3 + \frac{d_1}{1+c_{14}d_1} u_4(t-\tau), \tag{4c}$$

$$\frac{dx_4}{dt} = \frac{c_{11}c_{14}}{1+c_{14}d_1} x_3 + \frac{1}{1+c_{14}d_1} u_4(t-\tau) - c_{12} d_2 u_1 x_4, \tag{4d}$$

$$y_1 = T_{\mathrm{f}} = x_1, \tag{4e}$$

$$y_2 = T_{\mathrm{sz}} = x_2, \tag{4f}$$

$$y_3 = x_{\mathrm{O_2fg}} = \frac{-c_{15} d_2 u_1 x_4 + c_{16} u_3}{c_{17} x_3 + c_{18} d_2 u_1 x_4 + c_{19} u_3}, \tag{4g}$$

$$y_4 = \lambda_{\mathrm{fb}} = \frac{c_{16}(u_1 - c_{19})}{c_{15} d_2 u_1 x_4}. \tag{4h}$$

Here c_i are constant positive parameters. A tilde denotes slowly time-varying positive parameters.

IV. CONTROLLER DESIGN AND STABILITY ANALYSIS

Due to the time-delay of the actuating signal u_4 only the inputs u_1, u_2 and u_3 are used for input-output-linearization. Consequently only three output variables are controlled using this technique. Thus, the non-measurable output $y_4 = \lambda_{\mathrm{fb}}$ is neglected in a first step. The relative degree of system (4) is then given by $\{0\ 1\ 1\}$. Hence, the total relative degree equals 2 and leads to an internal dynamics of second order. The actuating signals u_1, u_2 and u_3 can be chosen such that the desired input-output dynamics

$$\frac{dy_1}{dt} = \beta_1(v_1 - y_1), \tag{5a}$$

$$\frac{dy_2}{dt} = \beta_2(v_2 - y_2), \tag{5b}$$

$$y_3 = v_3 \tag{5c}$$

is satisfied. Therein v_1, v_2 and v_3 are regarded as auxiliary input variables and β_1 and β_2 are positive constant controller parameters. The system state required for the resulting control law is estimated by an extended Kalman filter as it is described in [11], [16]. With the new state variables

$$\begin{bmatrix}\xi_1\\ \xi_2\end{bmatrix} = \begin{bmatrix}x_1\\ x_2\end{bmatrix} \quad \text{and} \quad \begin{bmatrix}\eta_1\\ \eta_2\end{bmatrix} = \begin{bmatrix}x_3\\ x_4\end{bmatrix} \tag{6}$$

the controlled system can be represented in Byrnes Isidori form i.e.

$$\frac{d}{dt}\begin{bmatrix}\xi_1\\ \xi_2\\ \eta_1\\ \eta_2\end{bmatrix} = \begin{bmatrix}\beta_1(v_1-\xi_1)\\ \beta_2(v_2-\xi_2)\\ q_1(\eta_1,u_4)\\ q_2(\eta_1,\xi_1,\xi_2,v_1,v_2,v_3,u_4)\end{bmatrix}. \tag{7}$$

Note that the actuating signal u_4 appears as input variable of the internal dynamics represented by the state variables η_1 and η_2. For any operating point $\xi_1 = v_1 = \text{const}$, $\xi_2 = v_2 = \text{const}$ and $v_3 = \text{const}$ the zero dynamics reads as

$$\frac{d}{dt}\begin{bmatrix}\eta_1\\ \eta_2\end{bmatrix} = \begin{bmatrix}-a_1(d_1) & 0\\ a_2(d_1,v_3) & 0\end{bmatrix}\cdot\begin{bmatrix}\eta_1\\ \eta_2\end{bmatrix} + \begin{bmatrix}b_1(d_1)\\ b_2(d_1)\end{bmatrix}u_4(t-\tau) + \begin{bmatrix}0\\ 1\end{bmatrix}\theta(v_1,v_2,v_3,d_3,d_4), \tag{8}$$

with the positive parameters a_1, a_2, b_1 and b_2 and the bounded function θ stated in the appendix. Because this zero dynamics is not asymptotically stable the input signal u_4 is used for stabilization and additionally to control the fourth output variable $y_4 = \lambda_{\text{fb}}$. For this purpose a combination of feed-forward and feedback control is proposed, see Fig. 2. The feed-forward component $u_{4,\text{eq}}$ of the input signal u_4 is computed such that the system remains at its desired steady-state $x_{4,\text{eq}} = \eta_{2,\text{eq}}$. The values $x_{4,\text{eq}}$ and $u_{4,\text{eq}}$ are determined by an equilibrium point calculation of model (4) with the desired output values $\mathbf{y}_\text{d} = \begin{bmatrix}y_{1,\text{d}} & y_{2,\text{d}} & y_{3,\text{d}} & y_{4,\text{d}}\end{bmatrix}^T$ and the current disturbance values $\mathbf{d} = \begin{bmatrix}d_1 & d_2 & d_3 & d_4\end{bmatrix}^T$. Thus it is possible to give a desired value $y_{4,\text{d}}$ for the output $y_4 = \lambda_{\text{fb}}$ and to adapt the values $x_{4,\text{eq}}$ and $u_{4,\text{eq}}$ to the desired load of the plant. With the feedback control the steady-state $x_{4,\text{eq}} = \eta_{2,\text{eq}}$ is stabilized.

The parameters a_1, a_2, b_1 and b_2 of the zero dynamics (8) depend on the disturbance d_1 and in addition a_2 is dependent on the input value v_3. The dependency of parameter a_2 on the input value v_3 is arranged within the model inaccuracies and thus can be neglected[1]. Compared to the system dynamics of (8) the disturbance d_1 is slowly time-varying. Thus, the parameters are assumed to be constant[2] and the zero dynamics (8) in combination with the control law

$$u_4(s) = R(s)\left[x_{4,\text{eq}}(s) - \eta_2(s)\right] + u_{4,\text{eq}}(s) \tag{9}$$

can be regarded as a linear and time invariant system with bounded inputs θ, $x_{4,\text{eq}}$ and $u_{4,\text{eq}}$. For stability analysis the inputs are neglected and the differential equations are transformed into the Laplace domain i.e.

$$\eta_1(s) = \frac{1}{s+a_1}\left[\eta_{10} - b_1 R(s)\eta_2(s)e^{-s\tau}\right], \tag{10a}$$

$$\eta_2(s) = \frac{1}{s + R(s)\frac{b_2(s+a_1)+b_1a_2}{(s+a_1)}e^{-s\tau}}\left(\eta_{20} + \frac{a_2}{s+a_1}\eta_{10}\right), \tag{10b}$$

[1]A variation of $v_3 = x_{\text{O}_2\text{RG}}$ within its maximum range given by $[0 \;\; 0.21]$ causes a variation of the parameter a_2 of about 1%.

[2]This assumption is necessary to enable the suggested way for the stability analysis. However, the influence of slow parameter variation (due to a variation of d_1) on the final results is discussed later.

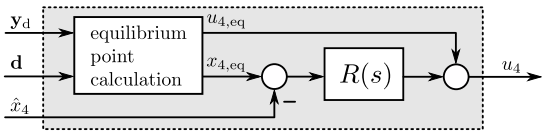

Fig. 2. Control structure for stabilization of the internal dynamics

with $\eta_{10} = \eta_1(t=0)$ and $\eta_{20} = \eta_2(t=0)$. Provided that $R(s)$ is a BIBO-stable transfer function the states η_1 and η_2 remain bounded if the transfer function

$$T(s) = \frac{\frac{1}{s}}{1 + R(s)\frac{b_2(s+a_1)+b_1a_2}{s(s+a_1)}e^{-s\tau}} \tag{11}$$

is BIBO-stable. To determine $R(s)$ the Nyquist stability criterion is used and the frequency response $L(j\omega)$ of the corresponding open loop transfer function

$$L(s) = R(s)b_2\frac{s + a_1 + a_2b_1/b_2}{s(s+a_1)}e^{-s\tau} \tag{12}$$

is investigated. Subsequently, two different structures for $R(s)$ are proposed.

The first idea is to use a proportional controller (P-controller) $R(s) = k_\text{p}$. For a special value of k_p the Nyquist plot $L(j\omega)$ is shown in principle in Fig. 3. The Nyquist stability criterion holds if the condition $0 < \kappa < 1$ is satisfied and thus if the positive parameter k_p is less than a maximum value $k_{\text{p,max}}$. Thereby κ is the intercept depicted in Fig. 3. As mentioned earlier the parameters a_1, a_2, b_1 and b_2 as well as the time-delay τ are dependent on the disturbance d_1. It can be shown that κ increases for increasing values of d_1. Thus κ is determined graphically for a maximum value $\hat{d}_1$ (with a maximum moisture content $\hat{w}_{\text{bm}}$ of the biomass). For $k_\text{p} = k_{\text{p,max}}$ the condition $-\kappa = -1$ holds and the maximum value $k_{\text{p,max}}$ can be derived. If the controller k_p is chosen according to $0 < k_\text{p} < k_{\text{p,max}}$ and the condition $d_1 < \hat{d}_1$ holds, the internal dynamics remains asymptotically stable.

In order to solve the problem of stabilization analytically the proportional controller is extended by a lead-controller (lead-lag compensator) given by

$$R(s) = k_\text{p}\frac{s+\omega_\text{n}}{s+\omega_\text{d}}. \tag{13}$$

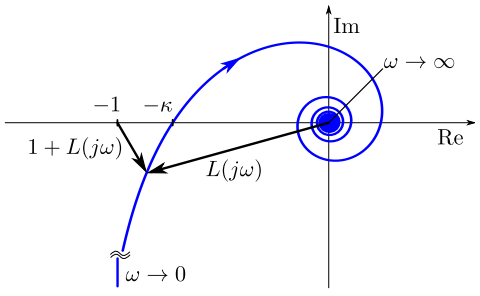

Fig. 3. Nyquist plot of the frequency response $L(j\omega)$

If the positive parameters ω_n and ω_d are chosen according to

$$\omega_\mathrm{n} = a_1 \qquad \text{and} \qquad \omega_\mathrm{d} = a_1 + a_2 b_1 / b_2 \tag{14}$$

the transfer function (12) is simplified and reads as

$$L(s) = \frac{k_\mathrm{p} b_2}{s} e^{-s\tau}. \tag{15}$$

Note that this compensation is possible only if the parameters a_1, a_2, b_1 and b_2 are constant. The case of time-varying parameters will be discussed later. For a special value of k_p the corresponding Nyquist plot $L(j\omega)$ looks as depicted in Fig. 3. The Nyquist stability criterion holds if the condition $0 < \kappa < 1$ is satisfied. Evaluating the frequency response $L(j\omega)$ of (15) for $\omega_0 = \frac{\pi}{2\tau}$ and $k_\mathrm{p} = k_\mathrm{p,max}$ yields

$$L(j\omega_0) = -k_\mathrm{p,max} \frac{2 b_2 \tau}{\pi} = -\kappa \stackrel{!}{=} -1. \tag{16}$$

So the maximum value $k_\mathrm{p,max}$ is calculated by

$$k_\mathrm{p,max} = \frac{\pi}{2 b_2 \hat{\tau}}, \tag{17}$$

where $\hat{\tau} = \tau(\hat{d}_1)$ is the maximum value of the time-delay τ determined for a maximum value $\hat{d}_1$ (with a maximum moisture content $\hat{w}_\mathrm{bm}$ of the biomass). If the parameters ω_n and ω_d of transfer function (13) are chosen according to (14), the parameters a_1, a_2, b_1 and b_2 are assumed to be constant and k_p is chosen according to $0 < k_\mathrm{p} < k_\mathrm{p,max}$ the internal dynamics is asymptotically stable.

Due to unknown variations of the disturbance d_1 the real parameters a_1, a_2, b_1 and b_2 differ from the values used for selecting ω_n and ω_d according to (14). Hence, expression (15) for the open loop transfer function (12) will not be achieved. However, if the parameters $\hat{a}_1$, $\hat{a}_2$, $\hat{b}_1$ and $\hat{b}_2$ are calculated using the maximum value $\hat{d}_1$ (with a maximum moisture content $\hat{w}_\mathrm{bm}$ of the biomass) and the parameters ω_n and ω_d are chosen according to

$$\omega_\mathrm{n} = \hat{a}_1 \qquad \text{and} \qquad \omega_\mathrm{d} = \hat{a}_1 + \hat{a}_2 \hat{b}_1 / \hat{b}_2 \tag{18}$$

a stability margin is achieved for disturbance values $d_1 < \hat{d}_1$ (respectively $w_\mathrm{bm} < \hat{w}_\mathrm{bm}$). Fig. 4 shows the frequency response of the open loop transfer function (12) with the controller (13) and the parameters (17) and (18) for different moisture contents w_bm. The control parameters are determined for the moisture content $\hat{w}_\mathrm{bm} = 0.5$. For decreasing moisture contents the same controller results an increasing phase margin of $L(j\omega)$ (see Fig. 4). Hence, the internal dynamics is asymptotically stable for $d_1 < \hat{d}_1$ (respectively $w_\mathrm{bm} < \hat{w}_\mathrm{bm}$).

In summary the control concept consists of a state controller for input-output-linearization, the investigated stabilization method and a Kalman filter for state estimation. Additionally PI-controllers are used to eliminate the steady-state control errors for the measured outputs y_1, y_2 and y_3. The structure of this concept is depicted in Fig. 5. There the vectors $\mathbf{v} = \begin{bmatrix} v_1 & v_2 & v_3 \end{bmatrix}^T$, $\hat{\mathbf{x}} = \begin{bmatrix} \hat{x}_1 & \hat{x}_2 & \hat{x}_3 & \hat{x}_4 \end{bmatrix}^T$, $\mathbf{u} = \begin{bmatrix} u_1 & u_2 & u_3 & u_4 \end{bmatrix}^T$ and $\mathbf{y}_\mathrm{m} = \begin{bmatrix} y_1 & y_2 & y_3 \end{bmatrix}^T$ are introduced.

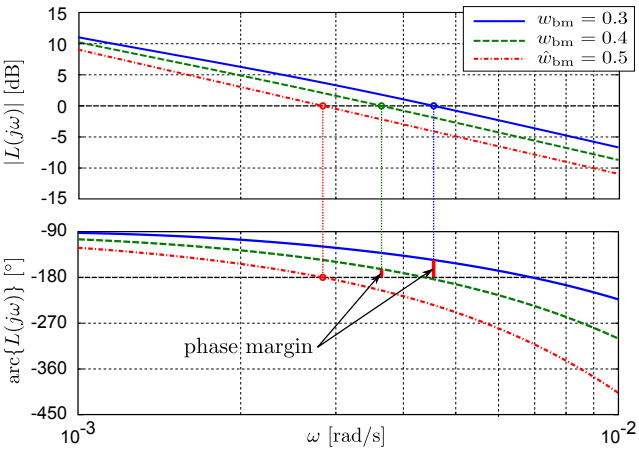

Fig. 4. Frequency response of the open loop transfer function $L(j\omega)$

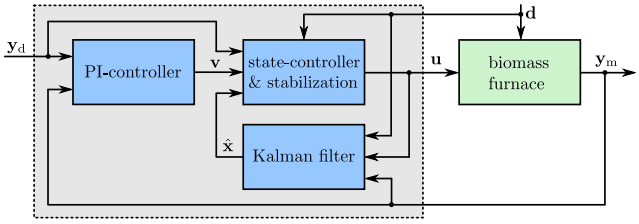

Fig. 5. Overall control structure of the proposed concept

V. RESULTS

The proposed control strategy is implemented on a medium-scale biomass furnace with a nominal boiler capacity of 180kW. To select the controller parameters and to show the behavior of the two suggested stabilization methods simulation studies are performed. The model parameters are found by experiments. The parameters $k_\mathrm{p,max}$ for the proportional controller as well as $k_\mathrm{p,max}$, ω_n and ω_d for the lead-controller are determined for a moisture content of $\hat{w}_\mathrm{bm} = 0.5$. The final parameters $k_\mathrm{p} = 0.5 k_\mathrm{p,max}$ are found via simulation studies. The parameters of the state-controller β_1 and β_2 are chosen such that the actuating signals do not saturate for common characteristics of the desired outputs and the disturbances. All parameters are summarized in Table I. In order to demonstrate the performance of the controlled plant an increase of the return temperature T_r from 70°C to 76°C resulting in a load change from 180kW to 120kW will be discussed (see Fig. 7 subplot 4). The water massflow $d_3 = \dot{m}_\mathrm{w} = 2.4$kg/s as well as the desired values

TABLE I
CONTROLLER PARAMETERS

	parameter	value
P-controller	k_p	0.0020 1/s
Lead-controller	k_p	0.0045 1/s
	ω_n	0.0012 rad/s
	ω_d	0.0033 rad/s
State-controller	β_1	0.0083 1/s
	β_2	0.0083 1/s

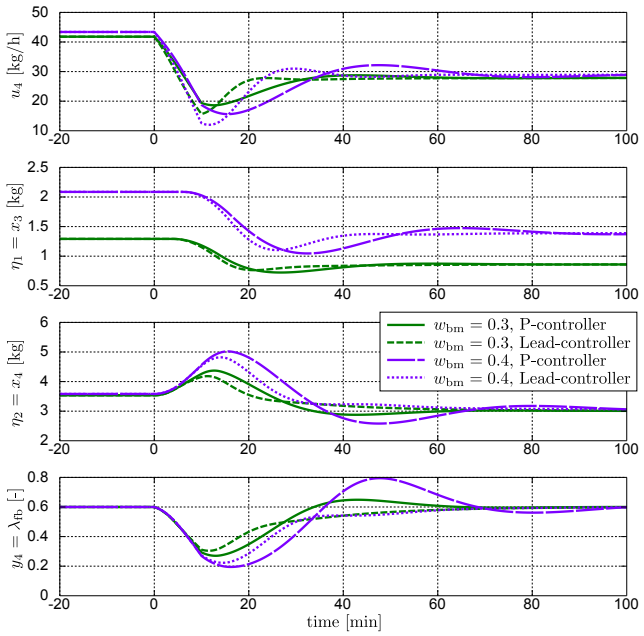

Fig. 6. Simulation results - comparison of the methods for stabilization of the internal dynamics for a load change from 180kW to 120kW at time $t = 0$

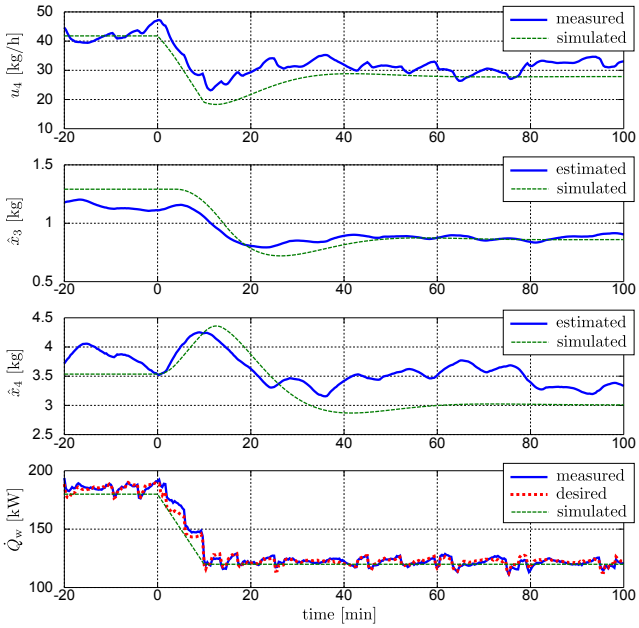

Fig. 7. Experimental results - the states x_3 and x_4 of the internal dynamics are stabilized by u_4 for a load change from 180kW to 120kW at time $t = 0$

$y_{1,\mathrm{d}} = 88°\mathrm{C}$, $y_{2,\mathrm{d}} = 1000°\mathrm{C}$, $y_{3,\mathrm{d}} = 7\%$ and $y_{4,\mathrm{d}} = 0.6$ remain constant.

A. Simulation

The simulations are based on model (4), where the disturbance $d_2 = 1$ is assumed to be constant. The simulation is performed for two different moisture contents $w_{\mathrm{bm}} = 0.3$ and $w_{\mathrm{bm}} = 0.4$ for both stabilization methods respectively. As a consequence of input-output-linearization the outputs $\mathbf{y}_{\mathrm{m}}$ track their constant desired values $y_{1,\mathrm{d}}$, $y_{2,\mathrm{d}}$ and $y_{3,\mathrm{d}}$ exactly. The results for the actuating signal $u_4 = \dot{m}_{\mathrm{ff}}$, the states of the internal dynamics η_1 and η_2 and the output $y_4 = \lambda_{\mathrm{fb}}$ are depicted in Fig. 6. For both moisture contents the feedback loop based on stabilization with the P-controller leads to an oscillating behavior for the states η_1 and η_2 and subsequently for the output y_4. Using the lead-controller for stabilization this oscillation is damped. Furthermore, the steady state behavior is reached in a shorter period of time. The discrepancy between the two stabilization methods decreases for smaller moisture contents. In summary both stabilization methods lead to a stable behavior of the internal dynamics.

B. Experiment

To control the outputs of the real biomass furnace the control structure depicted in Fig. 5 is implemented. Because the states are not completely measurable a Kalman filter is designed according to [16]. For the stabilization of the internal dynamics the proportional controller is used and the parameters listed in Table I are selected[3]. The used biomass fuel consists of wood chips with an average moisture content of $\bar{w}_{\mathrm{bm}} \approx 0.35$. Fig. 7 shows the results for the actuating signal $u_4 = \dot{m}_{\mathrm{ff}}$, the estimated internal states $\hat{x}_3$ and $\hat{x}_4$ and the heat flow transferred to the water circuit $\dot{Q}_{\mathrm{w}}$ in comparison with the respective simulation results. The simulated and measured results show similar behavior. The estimated value $\hat{x}_4$ is appreciable higher than in simulation. This deviation is caused by offsets of the measured values $\mathbf{y}_{\mathrm{m}}$ used for estimating $\hat{x}_4$. The measured heat flow $\dot{Q}_{\mathrm{w}}$ tracks the desired value almost perfectly. Variations of the desired value are caused by fluctuations of the water massflow $\dot{m}_{\mathrm{w}}$ and the return temperature T_{r} used for calculation of $\dot{Q}_{\mathrm{w}}$.

The controlled outputs $\mathbf{y}$ are shown in Fig. 8. The measured values y_1, y_2 and y_3 track their desired values in a very satisfying manner. At time $t = 0$ - when the load change begins - there is an overshoot of 0.8°C of the measured feed temperature T_{f} and the measured flue gas temperature T_{sz} drops to about 970°C. Both deviations are relatively small confirming the good control performance. The measured oxygen content $x_{\mathrm{O_2fg}}$ of the flue gas matches its desired value without any appreciable reaction. The steady state behavior of all measured values is very satisfying. The value $y_4 = \lambda_{\mathrm{fb}}$ was estimated with the help of the oxygen content $x_{\mathrm{O_2fg}}$ of the flue gas and the relation between primary and secondary air massflow. The variations of λ_{fb} are caused by the disturbance d_2 describing the variable decomposition factor of the combustion in the fuel bed. However, the deviation of the estimated value to the desired value is within an acceptable range. Due to the time-delay τ in the actuating signal u_4 this deviation cannot be completely eliminated.

[3]Due to limited access to the investigated biomass furnace it was not possible to test the stabilization with the lead-controller in experiment.

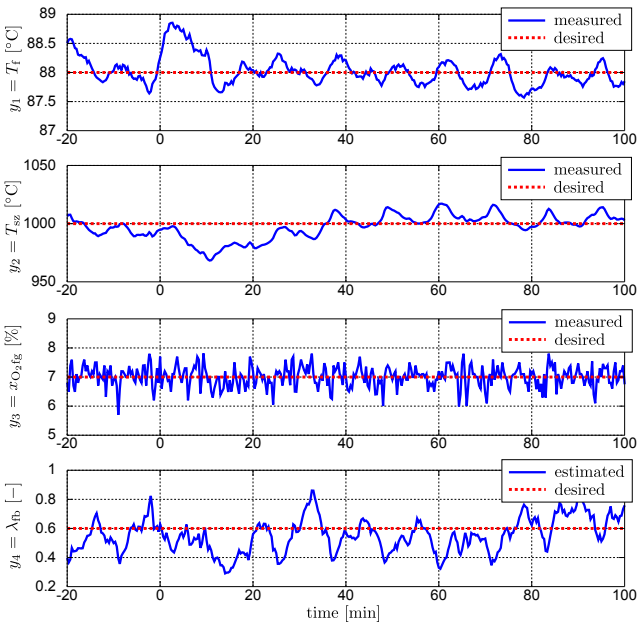

Fig. 8. Experimental results - controlled outputs for a load change from 180kW to 120kW at time $t = 0$

VI. CONCLUSION

The scope of the paper is the controller design for a biomass furnace based on input-output-linearization. Two methods for stabilization of the second order internal dynamics are discussed. For stability analysis the Nyquist stability criterion is used. Both stabilization strategies, a proportional controller as well as a lead-controller result in a stable closed loop behavior also for different moisture contents of the biomass. In experiment the stabilization of the internal dynamics with the proportional-controller results in good control performance of all four outputs. In particular using the discussed methods for stabilization fast convergence of the internal states is achieved. Finally, the resulting control performance of the air-ratio in the fuel bed leads to low emission operation and enables fast load changes.

APPENDIX

The parameters of the zero dynamics are calculated as follows:

$$a_1 = \frac{c_{11}}{1 + c_{14} d_1} \tag{19a}$$

$$\begin{aligned} a_2 = {} & \frac{c_{11} c_{14}}{1 + c_{14} d_1} + (c_{12}(c_{17}(\tilde{c}_{10}\tilde{c}_4 + \tilde{c}_{13}(\tilde{c}_4 - \tilde{c}_5) - \tilde{c}_5\tilde{c}_9)v_3 + \\ & (\tilde{c}_4(c_{11}\tilde{c}_{13} - c_7) - \tilde{c}_2(\tilde{c}_{13} + \tilde{c}_9))(c_{16} - c_{19}v_3)))/ \\ & ((\tilde{c}_{10}\tilde{c}_4 + \tilde{c}_{13}(\tilde{c}_4 - \tilde{c}_5) - \tilde{c}_5\tilde{c}_9)(c_{15} + c_{18}v_3) - \\ & (\tilde{c}_{13}(\tilde{c}_3 - c_{12}\tilde{c}_4) - \tilde{c}_4 c_8 + \tilde{c}_3\tilde{c}_9)(c_{16} - c_{19}v_3)) \end{aligned} \tag{19b}$$

$$b_1 = \frac{d_1}{1 + c_{14} d_1} \tag{19c}$$

$$b_2 = \frac{1}{1 + c_{14} d_1} \tag{19d}$$

$$\begin{aligned} \theta = {} & (c_1 c_{12} d_3 (d_4 - v_1)(\tilde{c}_{13} + \tilde{c}_9 - c_6 v_2)(c_{16} - c_{19}v_3))/ \\ & ((\tilde{c}_{10}\tilde{c}_4 + \tilde{c}_{13}(\tilde{c}_4 - \tilde{c}_5) - \tilde{c}_5\tilde{c}_9 + (-\tilde{c}_4 + \tilde{c}_5)c_6 v_2) \\ & (c_{15} + c_{18}v_3) - (\tilde{c}_{13}(\tilde{c}_3 - c_{12}\tilde{c}_4) - \tilde{c}_4 c_8 + \\ & \tilde{c}_3\tilde{c}_9 - \tilde{c}_3 c_6 v_2 + c_{12}\tilde{c}_4 c_6 v_2)(c_{16} - c_{19}v_3)). \end{aligned} \tag{19e}$$

REFERENCES

[1] J. Good, *Verbrennungsregelung bei automatisch beschickten Holzschnitzelfeuerungen*. Juris Druck & Verlag, 1992, (Forschungsbericht Nr. 11, Laboratorium für Energiesysteme ETH Zrich).

[2] J. Good and T. Nussbaumer, "Efficiency improvement and emission reduction by advanced combustion control technique (ACCT) with co/lambda control and setpoint optimization," in *Biomass for Energy and Industry: European Conference and Technology Exhibition*, vol. 10. C.A.R.M.E.N., June 1998.

[3] M. Kaltschmitt and H. Hartmann, *Energie aus Biomasse*. Springer-Verlag, 2001.

[4] S. Zipser, *Beitrag zur modellbasierten Regelung von Verbrennungsprozessen*. Universitätsverlag Karlsruhe, 2004.

[5] M. Leskens, L. van-Kessel, and O. Bosgra, "Model predictive control as a tool for improving the process operation of MSW combustion plants," *Waste Management*, vol. 25, pp. 788–798, October 2005.

[6] N. Paces, A. Voigt, S. Jakubek, A. Schirrer, and M. Kozek, "Combined control of combustion load and combustion position in a moving grate biomass furnace," in *Mediterranean Conference on Control and Automation, Corfu, Greece*, vol. 19, June 2011, pp. 1447 – 1452.

[7] J. Kortela and S.-L. Jämsä-Jounela, "Model predictive control for biopower combined heat and power (CHP) plant," in *International Symposium on Process Systems Engineering*, vol. 11. Elsevier, 2012, pp. 435–439.

[8] J. Slotine and W. Li, *Applied Nonlinear Control*. Prentice Hall, 1991.

[9] H. Khalil, *Nonlinear Systems*. Prentice Hall, 2002.

[10] A. Isidori, *Nonlinear Control Systems*. Springer-Verlag, 1995.

[11] M. Gölles, R. Bauer, T. Brunner, N. Dourdoumas, and I. Obernberger, "Model based control of a biomass grate furnace," in *European Conference on Industrial Furnaces and Boilers*, April 2011.

[12] M. Gölles, S. Reiter, T. Brunner, N. Dourdoumas, and I. Obernberger, "Model based control of a small-scale biomass boiler," *Control Engineering Practice*, vol. 22, pp. 94–102, January 2014.

[13] C. Schörghuber, M. Gölles, N. Dourdoumas, and I. Obernberger, "Model based control of the secondary air massflow of biomass furnaces," *at – Automatisierungstechnik*, vol. 62, pp. 487–499, July 2014, (in German).

[14] R. Bauer, M. Gölles, T. Brunner, N. Dourdoumas, and I. Obernberger, "Modelling of grate combustion in a medium scale biomass furnace for control purposes," *Biomass and Bioenergy*, vol. 34, no. 4, pp. 417–427, 2010.

[15] R. Bauer, M. Gölles, T. Brunner, N. Dourdoumas, and I. Obernberger, "Dynamic modelling of the heat transfer in a gas tube heat exchanger," *at – Automatisierungstechnik*, vol. 56, no. October, pp. 513–520, 2008, (in German).

[16] R. Seeber, M. Gölles, T. Brunner, N. Dourdoumas, and I. Obernberger, "Improvement of a model based control strategy for biomass furnaces," *at – Automatisierungstechnik*, vol. 62, pp. 891–902, December 2014, (in German).